N87-22210

INFLUENCE OF DISK LEAKAGE PATH ON LABYRINTH SEAL INLET SWIRL RATIO

R. Gordon Kirk
Virginia Polytechnic Institute and State University
Blacksburg, Virginia 24061

The results of numerous investigators have shown the importance of labyrinth seal inlet swirl on the calculated dynamic stiffness of labyrinth seals. These results have not included any calculation of inlet leakage swirl as a function of geometry and sealing conditions of the given seal. This paper outlines a method of calculating the inlet swirl at a given seal by introducing a radial chamber to predict the gas swirl as it goes from the stage tip down to the seal location.

For a centrifugal compressor, this amounts to including the flow path from the impeller discharge, down the back of the disk or front of the cover, then into the shaft seal or eye packing, respectively. The solution includes the friction factors of both the disk and stationary wall with account for mass flow rate and calculation of radial pressure gradients by a free vortex solution.

The results of various configurations are discussed and comparisons made to other published results of disk swirl.

INTRODUCTION

Recent reports in the literature (1,2,3,4,5) have addressed the problem of calculating the rotordynamic coefficients for a labyrinth seal having a given inlet gas swirl, pressure drop, and resulting mass flow. The centrifugal design engineer has at his disposal from standard aerodynamic design codes the gas swirl and pressures at the impeller tip. The solution of the leakage gas path swirl and resulting pressure distribution is important not only for labyrinth seal coefficients but also for proper thrust balance calculations. This paper presents an approximate method of calculating these desired parameters using a modified version of the solution technique as proposed by Iwatsubo (1) and later extended by Childs and Scharrer (2). The extensions and modifications to the theory as outlined by (2) will be discussed in this paper.

The equations of the modified formulation have been incorporated into a single labyrinth seal analysis computer code to permit rapid evaluation of different design conditions. The accuracy of the reported solution technique will be compared to experimental and analytical solution results as reported in reference (6) and to the limit case condition of zero leakage (approximately zero for computer program results).

NOMENCLATURE

Values are given in both SI and U.S. Customary Units. The calculations were made in U.S. Customary Units.

b - tangential velocity ratio, $U/(r\omega)$

c_i - wall separation at i^{th} radial chamber and radial clearance for seal tooth, m (in)

H_i - height of i^{th} seal element tooth, m (in)

L_i - axial length of i^{th} seal chamber, m (in)

$\dot{m}$ - mass flow rate, Kg/sec (lbm/sec)

P - gas pressure, N/m^2 (lb_f/in^2)

r - radial position on disk, m (in)

R, R_o - outer radius of disk, m (in)

R - gas constant, ($lb_f \cdot ft/lbm/^oR$)

RM - mean chamber radius, m (in)

RR - average radius of rotor seal chamber surface area, m (in)

RS - average radius of stator seal chamber surface area, m (in)

R_e - disk Reynolds number, $= R_o^2\omega/\nu$

s - wall separation, m (in)

S - separation ratio, $= s/R_o$

SJ - leakage parameter, $= Vs/(R_o^2\omega)$

T - gas absolute temperature, ^oK (^oR)

U_t - tangential velocity, m/sec (in/sec)

V_r - radial velocity, m/sec (in/sec)

Z - gas compressibility

ρ - gas density, Kg/m^2 (lbm/in^2)

τ_{rw} - radial wall shear stress, N/m^2 (lbf/in^2)

τ_{rd} - radial disk shear stress, N/m^2 (lbf/in^2)

ν - gas kinematic viscosity, m^2/sec (in^2/sec)

χ - position factor, $= (R_o - r)/R_o$

ω - rotor (disk) angular spin velocity, sec^{-1}

ω_β - swirl velocity for free vortex, sec^{-1}

METHOD OF SOLUTION

The solution technique proposed was developed to permit the same basic theory and computer code to calculate both the circumferential swirl and pressure distribution down the disk and across the labyrinth as one coupled system. This technique was initially intended as a quick first pass method but the results have proven to be very close to the more exact theories such that the added complication of coupling different theories and matching boundary conditions of pressures, temperatures, flows, and swirls may not be justified for rotordynamic evaluations. A typical configuration is shown in Figure 1 for a centrifugal compressor stage disk cover leakage flow path.

For the radial direction down the disk leakage path the equilibrium equation is given by the following equation (6):

$$-V_r \frac{dV_r}{dr} - \frac{U_t^2}{r} = -\frac{1}{\rho}\frac{dP}{dr} + \frac{\tau_{rw}}{\rho s} \pm \frac{\tau_{rd}}{\rho s} \qquad [1]$$

For a free vortex flow neglecting the radial shear force which will be accounted for by the crossflow factor in the circumferential equations, the pressure distribution equation becomes

$$\frac{dP}{dr} = \frac{\rho (r\omega_\beta)^2}{r} \qquad [2]$$

or

$$\frac{dP}{dr} = \rho r \omega_\beta^2 \qquad [3]$$

where

ω_β = gas swirl angular velocity at the radius, r.

Therefore, the pressure at any radius r is given by

$$P(r) = P(R) - \rho \frac{\omega_\beta^2}{2}(R^2 - r^2) \qquad [4]$$

This equation predicts the pressure along the disk if the gas swirl is known. The gas swirl can be calculated from the circumferential momentum equation as outlined in (2) and further modified to the following equation to account for variation in rotor, stator and mean flow chamber radius. In addition, the crossflow turbulence correction factors may be included in the solution to account for the inward flow resistance.

$$\frac{\dot{m}}{2\pi R_M}(Vo_i - Vo_{i-1}) = \frac{1/2\, Po_i}{ZRT_i}(R\omega - Vo_i)^2 * YNR * \left(\frac{|R\omega - Vo_i|DHY}{\nu}\right)^{YMR} \qquad [5]$$

$$* ARL * \text{sign}(R\omega - Vo_i) * \frac{RR}{RM} * C3$$

$$- 1/2\, \frac{Po_i}{ZRT_i} Vo_i^2 * YNS * \left(\frac{|Vo_i| * DHY}{\nu}\right)^{YMS} * ASL * SIGN(Vo_i) * \frac{RS}{RM} * C4$$

where

RM = mean chamber radius

RR = mean rotor surface radius

RS = mean stator surface radius

C3, C4 = crossflow turbulence factors

$Vo_i = RM_i \, \omega_{\beta i}$ = average chamber swirl velocity

DHY = hydraulic diameter of chamber

YNR, YNS, YMR, YMS = turbulence factors per reference (2)

ARL, ASL = shear area for rotor and stator

$\frac{P_{oi}}{ZRT_i}$ = pressure and temperature dependent gas density in i^{th} chamber

ν = gas kinematic viscosity

The leakage flow, $\dot{m}$, can be calculated as outlined in (2) or by other suitable calculations with the modification to radial chamber pressures given by equation (4).

The solution process requires that an initial swirl be selected to calculate the pressure field and leakage. A swirl of 50% is suggested for starting the solution. With this pressure field and flow, the momentum equation given by Eq. (5) is solved for the first pass swirl values. These swirl values are then used to recalculate the pressure drops down the disk and through the labyrinth and the resulting flow. Another pass through Eq. (5) solution yields the second pass swirl values. Typically, three passes give the desired convergence and the inlet swirl to the labyrinth is then taken from the chamber ahead of the first sealing tooth.

A general geometry input is used such that for the radial chambers a very small tooth height and length with a tooth clearance equal to the disk to wall spacing can be used to model the flow path. The radial surface area is calculated using the indicated radius of each tooth location.

RESULTS OF SWIRL PREDICTED IN GAS LEAK PATH

The evaluation of the proposed swirl calculation procedure has been based upon numerous similar conditions as reported by Jimbo (6). Initial comparisons of actual compressor swirl results from similar geometry is overplotted in Fig. 2. The parameter for leakage flow was noted to be similar to those given by Jimbo. The leakage flow parameter is defined as

$$SJ = \frac{V}{R_o \omega} * \frac{s}{R_o} \qquad [6]$$

where

V = radial gas velocity

R_o = disk outer radius

ω = rotor speed

s = wall separation

For SJ = 0.0002 it is obvious that the compressor disk swirl does not agree with the reported complete analytical solution. The swirl rates are greater from the labyrinth program approximate solution. However, the other parameter, the disk Reynolds number given by

$$Re = R_o^2 \, \omega/\nu \qquad [7]$$

was calculated and found to be considerably different from the test results. The analysis results by Jimbo used air and a $R_e = 9.82 \times 10^5$ was quoted. These initial compressor test results had an $R_e = 1.1 \times 10^8$. To match the parameters for the two systems the gas, pressure drop, and rotor speed were changed as given in Table 1 under test rig conditions. This gave a disk Reynolds number of $R_e = 3 \times 10^6$, only off by a factor of 3 from Jimbo, compared to a factor of 112 for the compressor stage results.

The results for the labyrinth analysis overplot to the accuracy that the curves can be evaluated. The swirl results for the compressor stage and the test result condition are given in Tables 2 and 3, respectively. The swirl down the disk and through the labyrinth are given in the table with the radius χ-position factor indicated for comparison to the analysis results of Figure 2. The results are in excellent agreement for the case of near zero flow (i.e., swirl ~0.5) and for SJ = 0.0002 where the swirl at χ-position factor of 0.31 is now calculated as 0.563 as compared to 0.63 for the compressor gas. A comparison of the compressor swirl, test case calculation, Jimbo calculation, and test results reported by Jimbo are shown in Figure 3. The test results show a slowing of the swirl that is not predicted. The test rig was equiped with numerous flow and pressure measuring ports in the stator wall and it is very possible that the cause of the test rig result reduced swirl was the increased surface roughness resulting from the measuring instruments. Complex flow fields could also be the cause of the discrepancy and are beyond the scope of the present analysis. Results for reduced leakage, SJ = .000052, are given in Fig. 4 and labyrinth analysis compressor results for SJ = .0000372 overplotted. This case of reduced leakage compares closely even though the disk Reynolds numbers are not similar. The test rig results once again show a reduced swirl ratio with great restriction noted in the χ-position factor range of 0.4-0.5. The overall trend is similar as concluded by Jimbo.

One additional labyrinth program result is given in Table 4 for the condition of leakage from the final compressor stage through a balance piston full labyrinth. These results have a wall spacing that reduces as the radius reduces. A swirl of 0.82 is predicted for this geometry and gas properties, even though the flow SJ parameter is 0.00021 and a uniform spacing air test result would give a swirl rate closer to 0.6 (see Fig. 2 for χ-position ~0.4).

CONCLUSIONS

(1) The proposed approximate calculation procedure produces results that are acceptable for rotor dynamic evaluations of labyrinth seals.

(2) The flow parameter, SJ, and disk Reynolds number, Re, used by Jimbo to present results are very useful in comparing results for different designs and give great insight into disk swirl behavior.

(3) Non-uniform leak path geometry can be used to increase or decrease the swirl in the gas leak path.

(4) Increased stator surface roughness will suppress the swirl due to the increased shear drag on the swirling flow.

RECOMMENDATIONS

(1) Test evaluations using current technology flow measurement capability should be conducted on typical compressor and turbine disk design gas leak path configurations.

(2) The importance of gas properties and actual system configurations must be closely evaluated.

(3) The proposed calculation procedure can be used, with a high degree of confidence, for entry swirl evaluation of compressor labyrinth designs.

REFERENCES

(1) Iwatsubo, T., N. Matooka, and R. Kawai, "Spring and Damping Coefficients of the Labyrinth Seal," NASA CP 2250, 1982, pp. 205-222.

(2) Childs, D. W., and J. K. Scharrer, "An Iwatsubo-Based Solution for Labyrinth Seals - Comparison to Experimental Results," Rotordynamic Instability Problems in High Performance Turbomachinery - 1984, Texas A&M University, College Station, Texas, May 28-30, 1984.

(3) Benckert, H., and J. Wachter, "Flow Induced Spring Coefficients of Labyrinth Seals for Application in Rotordynamics," NASA CP 2133 Proceedings of a Workshop held at Texas A&M University May 12-14, 1980, Rotordynamic Instability Problems of High Performance Turbomachinery, pp. 189-212.

(4) Jenny, R., "Labyrinths as a Cause of Self-Excited Rotor Oscillations in Centrifugal Compressors," Sulzer Technical Review 4, 1980, pp. 149-156.

(5) Kirk, R. G., "Evaluation of Aerodynamic Instability Mechanisms for Centrifugal Compressors," ASME Paper 85-DET-147. Presented at Design Engineering Vibration Conference, Cincinnati, Ohio, September 10-13, 1985.

(6) Jimbo, H., "Investigation of the Interaction of Windage and Leakage Phenomena in a Centrifugal Compressor," ASME Paper 56-A-47, presented at ASME Annual Meeting, New York, NY, July 30, 1956.

TABLE 1 SYSTEM PARAMETERS FOR ACTUAL COMPRESSOR STAGE DESIGN CONDITIONS AND AN ASSUMED SYSTEM TO APPROXIMATE THE RESULTS OF TEST CONDITIONS FROM REFERENCE 6.

PARAMETER	COMPRESSOR STAGE	TEST RIG CONDITIONS (Ref. 6 assumed conditions)
MW	21.33	25.95
ν, m^2/s (in^2/sec)	2.79×10^{-7} (4.32×10^{-4})	4.64×10^{-6} (7.19×10^{-3})
Z	.89	.955
PS, N/m^2) (lb/in^2)	5.90×10^6 (855)	3.43×10^5 (49.7)
PE, N/m^2 (lb/in^2)	5.17×10^6 (750)	1.01×10^5 (14.7)
T, ^oK (^oR)	331.6 (602.9)	301.4 (548.5)
N, Hz (RPM)	207.4 (12566)	100.0 (6000)
R_o, m (in)	.154 (6.05)	.154 (6.05)
R_e	1.1×10^8	3×10^6

TABLE 2 RESULTS FOR COMPRESSOR STAGE GIVING PREDICTED CHAMBER FLOW SWIRL RATIO

CHAMBER	χ	SJ = 0.000023	0.00014	0.000236	0.00034
DISK TIP	0	.52	.52	.52	.52
2	.08	.5033	.534	.548	.557
3	.17	.5053	.5496	.571	.5867
4	.25	.5095	.5689	.600	.6225
5	.31	.5144	.5938	.632	.6603
RADIAL ↑ 6	.34	.5045	.5997	.6425	.6731
TURN 7	-	.452	.5605	.6111	.6472
SEAL 8	-	.384	.5121	.571	.6131
↓ 9	-	.359	.475	.5377	.5834
10	-	.350	.447	.5097	.5574
11	-	.346	.425	.4862	.5347
12	-	.345	.408	.4663	.5146

$$R_e = \frac{R_o^2 \omega}{\nu} = 1.1 \times 10^8$$

TABLE 3 RESULTS FOR TEST CASE GIVING PREDICTED CHAMBER SWIRL RATIO FOR ASSUMED SUPPLY PRESSURE CONDITIONS (SEE TABLE 1)

CHAMBER	χ	SJ = .000015	0.0001	0.00022	0.00034
Disk Tip	0	.52	.52	.52	.52
2	.08	.496	.509	.522	.534
3	.17	.496	.513	.532	.549
4	.25	.497	.519	.544	.567
5	.31	.492	.529	.563	.592
RADIAL ↑ 6	.34	.47	.524	.564	.597
TURN 7	-	.43	.473	.518	.558
SEAL 8	-	.3513	.4105	.465	.511
↓ 9	-	.3445	.3798	.431	.478
10	-	.3438	.364	.408	.453
11	-	.3438	.3558	.392	.434
12	-	.3438	.3512	.382	.421

$$R_e = \frac{R_o^2 \omega}{\nu} = 3 \times 10^6$$

TABLE 4 RESULTS OF LEAKAGE AND GAS SWIRL FOR FLOW FROM LAST STAGE TO A BALANCE PISTON LABYRINTH HAVING 15 TEETH

CHAMBER	χ (dim.)	SWIRL (dim.)	RADIUS (in.)	WALL SPACE (in.)
0	0	.637	9	-
1	.001	.641	8.94	.15
2	.07	.6756	8.34	.4
3	.15	.705	7.65	.36
4	.22	.732	7.02	.32
5	.293	.765	6.36	.3
RADIAL ↑ 6	.375	.81	5.62	.26
TURN 7	.42	.823	5.18	.22
SEAL ↓ 8	-	.781	5.14	-
9	-	.74	5.14	-
10	-	.71	5.14	-
11	-	.68	5.14	-
12	-	.66	5.14	-
13	-	.64	5.14	-
14	-	.62	5.14	-
15	-	.61	5.14	-
16	-	.598	5.14	-
17	-	.588	5.14	-
18	-	.580	5.14	-
19	-	.573	5.14	-
20	-	.567	5.14	-
21	-	.563	5.14	-

N = 11097. RPM
MW = 18.3
PS = 948 PSI
PE = 253 PSI
$\nu = 7.63 \times 10^{-4}$ in^2/sec
Z = 0.979
$\gamma = 1.255$
leakage = 1.09 lb$_m$/sec

SJ ≃ 0.00021

$$R_e = \frac{9^2(1162)}{7.63 \times 10^{-4}} = 1.23 \times 10^8$$

$C_p = 0.52$

c = 0.0115 in. radial clearance
type seal = interlocking

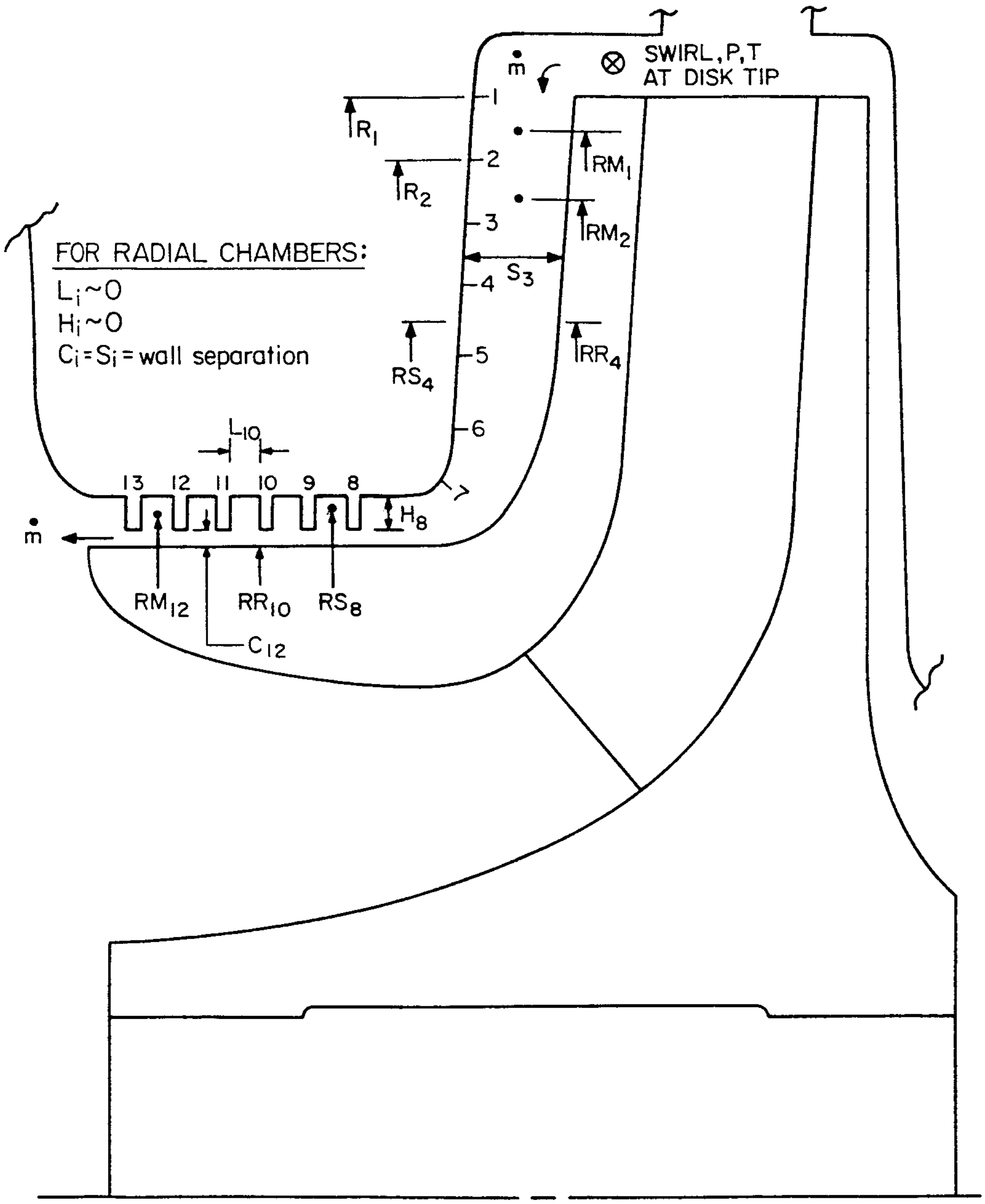

Figure 1. – Typical compressor stage showing disk cover gas leakage path with nomenclature for analysis.

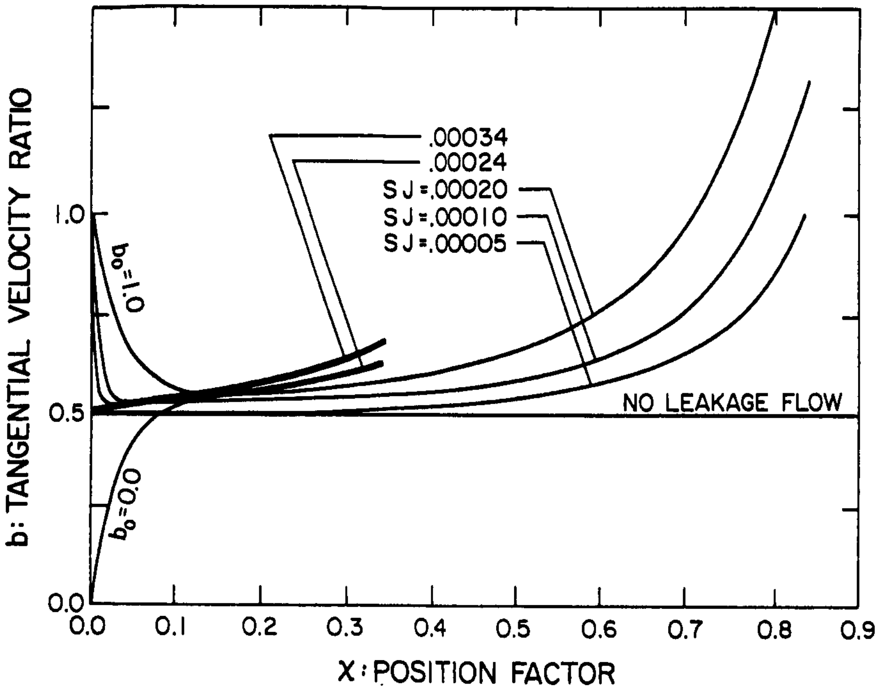

Figure 2. - Velocity profile along radius, $b = U/(r\omega)$ versus $\chi = (R_o-r)/R_o$ at $R_e = R_o^2\ \omega/\nu = 9.82\times10^5$. Overplot of typical compressor result with $R_e = 1.1\times10^8$ (From Jimbo - fig. 6 ref. (6)).

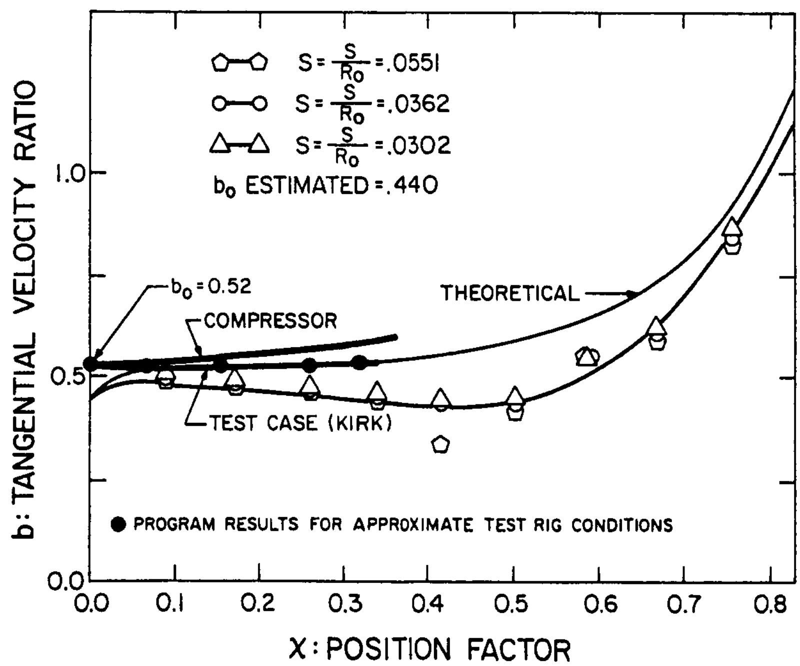

Figure 3. - Tangential velocity profile along radius $b = U/(r\omega)$ versus $\chi = R_o-r/R_o$ for constant leakage flow $SJ = (s/R_o)[V/R_o\omega)] = 0.000104$ at $R_e = 9.82\times10^5$. Overplot of a typical compressor result with $SJ = 0.00014$ and $R_e = 1.1\times10^8$; test case points for $SJ = 0.0001$ and $R_e = 3\times10^6$ (overplot on fig. 18 of ref. (6)).

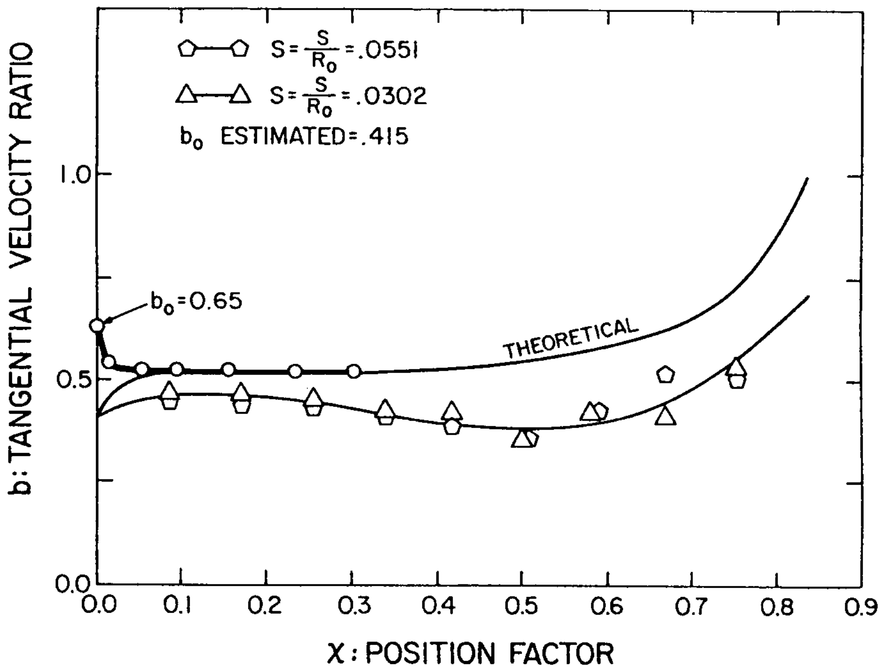

Figure 4. - Tangential velocity profile along radius $b = U/(r\omega)$ versus $\chi = R_o - r/R_o$ for constant leakage flow $SJ = (s/R_o)[V/(R_o\omega)] = 0.000052$ at $R_e = 9.82 \times 10^5$. Overplot of compressor having $SJ = 0.0000372$ and $R_e = 1.3 \times 10^8$ (overplot on fig. 20 of ref. (6)).